World Academy of Science, Engineering and Technology
International Journal of Electrical and Computer Engineering
Vol:2, No:7, 2008

Study and Enhancement of Flash Evaporation Desalination Utilizing the Ocean Thermocline and Discharged heat

Sami Mutair and Yasuyuki Ikegami

***Abstract*—**This paper reports on the results of experimental investigations of flash evaporation from superheated jet issues vertically upward from a round straight nozzle of 81.3 mm diameter. For the investigated range of jet superheat degree and velocity, it was shown that flash evaporation enhances with initial temperature increase. Due to the increase of jet inertia and subsequently the delay of jet shattering, increase of jet velocity was found to result in increase of evaporation "delay period". An empirical equation predicts the jet evaporation completion height was developed, this equation is thought to be useful in designing the flash evaporation chamber. In attempts for enhancement of flash evaporation, use of steel wire mesh located at short distance downstream was found effective with no consequent pressure drop.

***Keywords*—**Enhancement; Flash Evaporation; OTEC; superheated jet

I. Introduction

AS a result of the shortage of energy resources and the environmental pollution accompanying the combustion of fossil fuels to generate electricity and it's major contribution to the global warming problem, along with the scarcity of fresh water resource; energy and water issues are obtaining a considerable interest of researchers and concerning authorities likewise. Conversion of renewable energy resources is promoting and can solve the energy and environmental problems, while desalination of saline water bodies which form the majority of water resources on the earth can definitely substitute the shortage of fresh water. Ocean Thermal Energy conversion (OTEC) is one of the promising technologies to utilize the temperature difference between the hot shallow water and cold deep water of ocean to drive a certain power cycle and generate electricity, this process requires a huge quantity of both hot and cold water to be pumped from the ocean to supply the OTEC power plant; for the ultimate usage of this pumped water, desalination plant should be combined with the closed-cycle OTEC plant, where the discharged water from the electricity generation plant supply the flash evaporation based desalination plant. As the feed water temperature is low, evaporation process should be carried out under vacuum. This process can also be efficiently utilized in exploitation of the industrial discharged heat for the desalination of brackish or seawater and at the same time to cool down the devices. Miyatake et al. [1] experimentally investigated the spray flash evaporation phenomena occur when the sub-cooled water undergoes a sudden reduction of the surrounding pressure below the saturation pressure; experiments were done using a circular nozzle issuing the water downward at 60 degrees Celsius. Nozzles of different diameters were examined and the influence of superheat degree was clarified and considered as the driving force that controls the intensity of evaporation; Through this study, water temperature was found to undergo two exponential decays after the elapsing of a period of time named "Delay time"; variation of water temperature with time was correlated by an empirical equation assuming constant velocity of water jet at the area of influence. Through a comparison it was observed that the rate of flash evaporation of a liquid jet is extremely faster than those of flowing superheated liquid in conventional MSF evaporators and superheated pool water. Miyatake et al. [2] extended the study and investigated the influence of liquid temperature on the spray flash evaporation at temperatures of 40 and 80°C, from the experimental results, a more general empirical equation suitable for predicting the variation of liquid temperature in the center of jet with residence time was deduced. It was seen that, even at lower liquid temperatures, spray flash evaporation still had higher evaporation performance and faster evaporation rate than the flash evaporation occurring in other systems. However, Uehara et al. [3] have shown that correlations proposed by Miyatake et al. [2] is not applicable for jets at temperatures less than 40 0C and developed a new correlation for this purpose. Ikegami et al. [4] have investigated the influence of injection direction and confirmed that upwardly issuing jets have better performance and faster evaporation than those downwardly issuing jets due to the natural maxing effect occurs by the falling droplets; Muthunayagam et al. [5] studied the feasibility of desalination by low-pressure vaporization of seawater at temperatures between 26 and 32 °C at a pilot plant. The plant was operated at vacuum pressures between 1.3 and 2.3 KPa. The saline water was sprayed into the vaporizer as free droplets using a swirl

Sami Mutair is with the Graduate School of Science and Engineering, Saga University, 1-Honjo-machi, Saga city, Japan, 840-8502 phone: +81-952-28-8624; fax: +81-952-28-8595; e-mail: samymutair@ hotmail.com.

Yasuyuki Ikegami is with Institute of Ocean Energy, Saga University, 1-Honjo-machi, Saga city, Japan, 840-8502 phone: +81-952-28-8624; fax: +81-952-28-8595; e-mail: ikegami@ioes.saga-u.ac.jp.

nozzle. Condensation of the vapor so formed, was carried out in a shell and tube heat exchanger. Peter et al. [6] studied the phenomenon of flashing and shattering of superheat liquid jet in the field of low pressure. They described four physical characteristics of the jet in the area of low pressure and these are: non-shattering liquid jet, partially shattering liquid jet, completely shattering jet and flare flashing liquid jet. They studied temperature distribution at both the axial and radial directions along the liquid jet. They also studied the distribution of the droplet size and the contribution of bubble nucleation and growth to the liquid jet shattering in the area of low pressure. Brown and York [7] studied the sprays formed by flashing liquid jets issuing from rough orifices of sharp edge orifices. Liquids which are driven from a high pressure area to another one of low pressure often cross the equilibrium pressure for the liquid temperature and disintegrated into spray by partial evolution of vapor. Their study of the sprays from water and feron-11 jets analyzed drop sizes, drop velocities and spray patterns. The mechanism, which controls the process, was also analyzed. A critical superheat was found, where the jet of liquid was shattered by rapid bubble growth. Also the bubble growth rate was controlled with the Weber number, where its critical value for low viscosity liquid was 12.5, the mean drop size also correlated with the Weber number and the degree of superheat.

In this paper, flash evaporation occurs in the superheated water jet was experimentally investigated. Influence of flow velocity and initial water temperature was subject of interest. Enhancement of evaporation by means of steel wire meshes installed at several locations above the nozzle exit was also investigated.

II. Description of Phenomenon

Thermodynamically, flash evaporation occurs when a saturated liquid undergoes a sudden reduction in the surrounding pressure so that a part of the liquid immediately turns to vapor to regain equilibrium; under adiabatic conditions, the generated vapor receives its latent heat of vaporization at the expenses of the surrounding liquid and both the vapor and the residual liquid are cooled to the saturation temperature at the reduced pressure. In this research, tab water was injected vertically upward in a depressurized chamber through a round straight nozzles at various flow conditions; flash evaporation occurs at the active nucleation sites formed naturally by the turbulent mixing effects within the jet in addition to the small cavities exists at the inner nozzles surfaces with no attempts to induce swirl or nuclei in addition to that acquired by flow ordinarily. However, jets at superheat as low as two degrees reported partial shattering while at high degrees of superheat, bubble formation and growth starts earlier within the nozzle, resulting in greater bubble flow at the nozzle exit and thus, the flow of formed bubbles intensively shatters the liquid column near the exit into small spray and extends the interfacial area so that evaporation becomes more violent and the rate of temperature decline becomes faster.

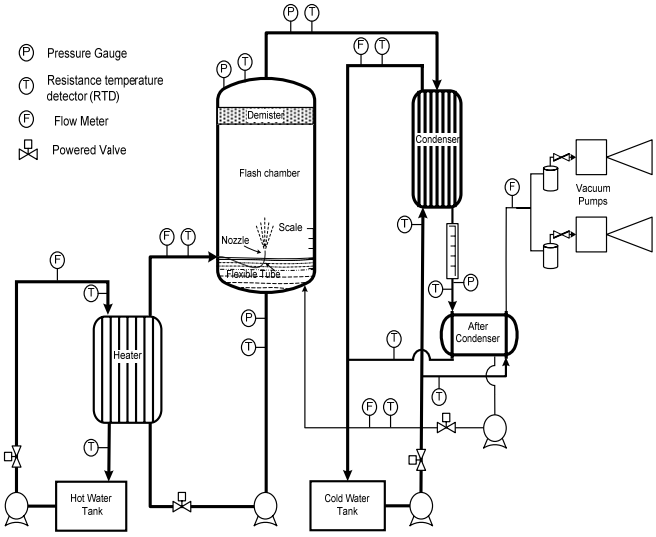

Fig.1 Layout of experimental setup

TABLE I
Range of Variables

Parameter	*Range*
Nozzle Diameter [mm]	81.3
Velocity, u [m/s]	0.8, 1.25, 2.21, 3.56
Initial temperature, T_0 [°C]	24, 30, 35, 40
Degree Superheat ΔT_s [°C]	2~8

III. Experimental Apparatus and Procedure

As shown in Fig.1, after sufficient duration of De-aeration, the tap water is continually heated in the heater and circulated in the low pressurized chamber, where the flash evaporation occurs and part of the water turns to vapor in order to regain equilibrium at the reduced pressure, the formed steam is drawn to the condenser, and then to the after condenser by the pressure gradient, where the majority of the vapor is condensed on the vertical plate type condenser, and the remaining small part of vapor is condensed in after condenser; the resulting distilled water is released from the low pressurized after condenser by downfall several meters below the after condenser level and then recycled in the flash evaporation chamber to maintain constant water level through the whole experiment duration. Two axial vacuum pumps are used to make the vacuum and connected to the after-condenser and condenser in series, respectively. Two separate loops of hot and cold water feed the heater and the condenser respectively; the cold water temperature was held constant at around 8 Celsius degrees through all experiment. Set of thermo-resistances, flow meters, and pressure gauges are installed at various locations to observe the experimental conditions. The temperature distribution of the water jet inside the chamber is measured by 20 thermo-resistances fixed on a horizontal steel bar, and movable a long the vertical axes to adjust the measurement level.

Containment of the dissolved gases in the test water was found to affect evaporation phenomena strongly and in order to obtain reliable and indicative results; all experiments were carried out at the absence of these gases where they were rejected from the test water by sufficient de-aeration under high temperature and low pressure. Influencing factors and their experimented range are given in table. 1

IV. Definition of Physical Quantities

$$\Delta T_s = T_0 - T_s \tag{1}$$

$$\theta_{(r,z)} = \frac{T_{(r,z)} - T_s}{T_0 - T_s} \tag{2}$$

$$H = c_{pL}(T_0 - T_s)/h_{fg} \tag{3}$$

$$We = \frac{\rho u^2 d}{\sigma} \tag{4}$$

The dimensionless temperature, θ introduced in (2) indicates the ratio of the superheat degree at a given location to the initial superheat degree ΔT_s defined at (1) where T_0 is initial water temperature measured in the compressed liquid region about 10 meters far from the flash evaporator inlet, T_s is the saturation temperature corresponds to the pressure inside the flash evaporator measured at the saturated bulk vapor; z is the vertical distance measured from the nozzle exit level and r is the horizontal distance measured from the center of the nozzle. The dimensionless number H, defined in (3) is a ratio of sensible to latent heat and it is a representative for the thermal properties of the water where c_{pL} is the specific heat at constant pressure, and h_{fg} is the latent heat of vaporization. In (4), Weber number, We which is a ratio of inertia to surface tension forces, interprets the dynamic properties of the flowing jet where u is velocity of injected water, d is the nozzle diameter, ρ_l and σ are density and surface tension of water, respectively.

V. Experimental Results and Discussion

A. Flow Modes

Through variety of experiments investigating temperature variation at the centerline of the jet, three flow zones were designated in the jet, each is of different characteristics namely:1-potential core zone; exists near the nozzle exit and mainly characterized by un-shattered flow and negligible temperature decline, 2- spray zone; through which, the jet shatters and diffuses in a conical shape so that the interface area extends and the water temperature declines rapidly and 3-Saturation zone; through which, temperature is relatively constant and the equilibrium condition is so far attained, Fig. 2-a shows the temperature profile at the jet axis at an arbitrary condition with the three flow zones indicated, while the isothermal diagram in Fig. 2-b shows the corresponding temperature distribution at the area of influence near the nozzle exit; each flow zone in Fig. 2-a has a correspondent thermal behavior in Fig. 2-b, the potential core zone , spray zone and saturation zone in Fig.2-a are represented by the continuous area near the nozzle exit, the adjacent isothermal lines and the widespread area in Fig. 2-b, respectively.

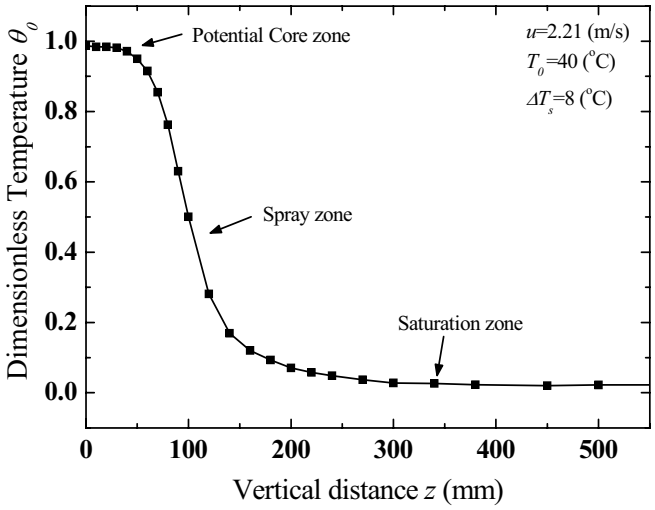

Fig. 2-a Dimensionless temperature profile at centerline of the jet

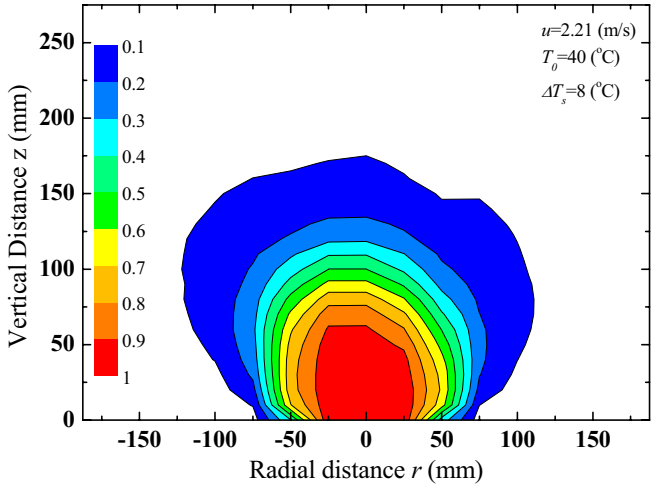

Fig. 2-b Isothermal diagram of temperature distribution near the nozzle exit

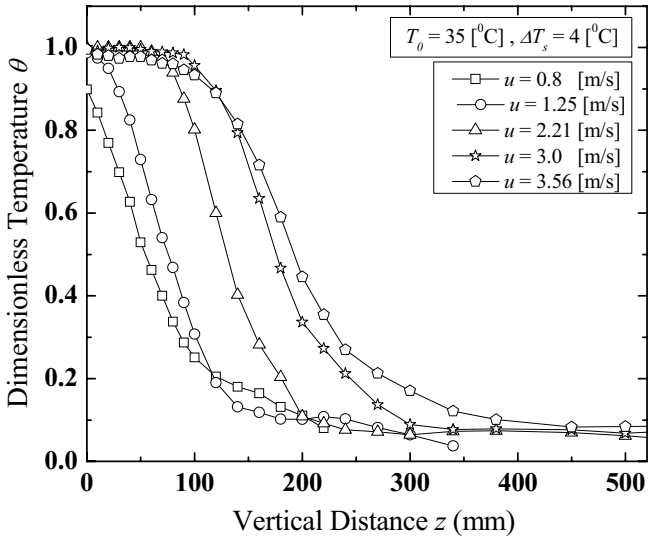

Fig. 3 Variation of θ with distance at various velocities

B. Influence of Flow Velocity

Velocity represents the retarding force tends to maintain the jet un-shattered. At constant temperature and degree of superheat, flow velocity is the main parameter influences the beginning point of each flow zone. The most significant influence of velocity appears at the first zone "liquid column zone" where the increases of velocity increases the height of water column, increase the static pressure and subsequently delays the initiation of spray zone resulting in increasing the overall vertical distance required for the completion of evaporation. Fig. 3 demonstrates the influence of velocity where temperature profiles at the centerline of the jet were obtained at various velocities while the other flow conditions were maintained constant.

C. Influence of Temperature

Through the shape of temperature profiles at the centerline of the jet indicated in Fig. 4 and obtained at different initial degrees, water initial temperature was found to enhance evaporation linearly when the other conditions are kept constant; temperature decrease or increase shifts the curves of θ - z horizontally and linearly to the right or left direction respectively i.e. the θ - z curves divide the normal line to any point located on these curves into intervals of length linearly proportional to the temperature differences between these curves, initial water increase results also in decrease of the value of the dimensionless temperature θ at the nozzle exit. Similar behaviour was observed when temperature profiles were drawn at different velocities and superheat degrees. In fig. 5, the vertical height z at which the water attains values of θ from 0.4 to 0.9 was measured and plotted against the water temperatures ranges from 24 to 40 degrees, these selected values of θ lie on the vapor-liquid spray zone, which involves the highest rate of evaporation and characterizes the whole phenomena. This graph shows that the vertical distance z required to attain a certain value of θ decreases linearly with the increase of temperature, i.e. in the vapor-liquid spray zone, evaporation at different temperatures happens at constant rate when other parameters remain constant.

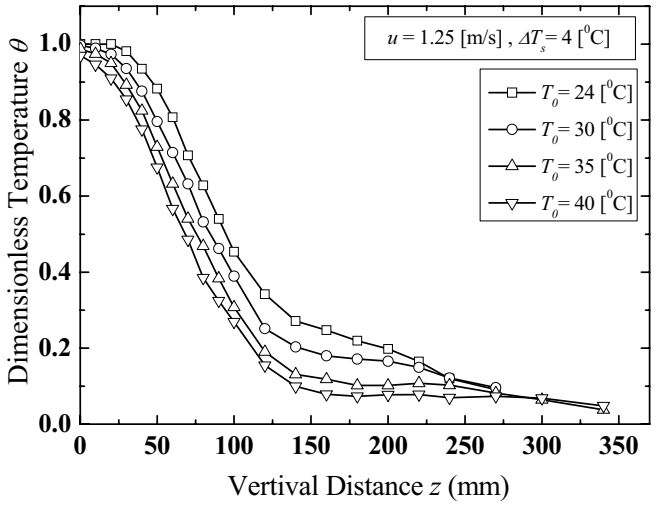

Fig. 4 Temperature profiles at different water temperature

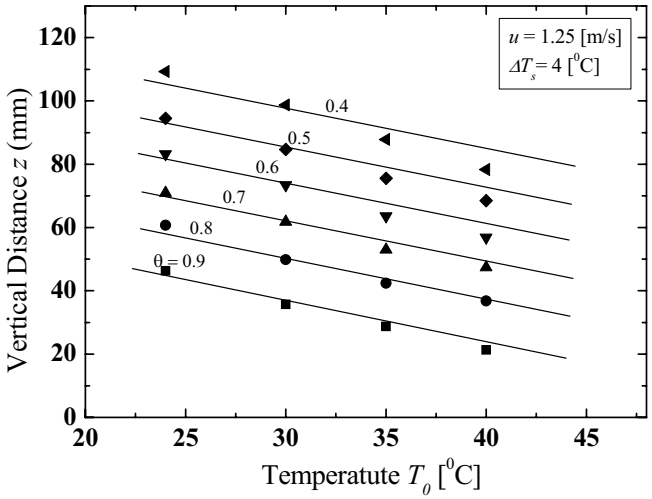

Fig. 5 Temperature effect on the height z required to attain values of θ in the vapor-liquid spray zone.

D. Actual and Theoretical Amount of Distilled Water

It was found that all the sensible heat consumed in the evaporation chamber is converted to latent heat to produce distilled water of temperature equals to saturation temperature. Then, the theoretical amount of produced distilled water, m_{DW} can be calculated from the heat balance equations as fellows:

$$m_{DW} = \frac{m_{FE} c_{pL} \Delta T_s}{h_{fg}} \quad (5)$$

Where, m_{FE} is the flow rate of water entering the flash evaporation chamber. The actual amount was measured directly by a sensitive flow meter installed in the fresh water recycling line connecting between the after condenser and the flash evaporation chamber, fig. 6 shows that actual and theoretical amounts matches well with the un-certainties doesn't increase 10%.

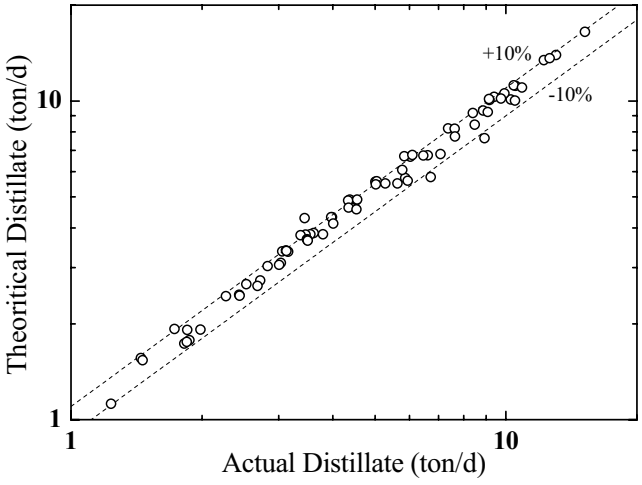

Fig. 6 Actual and theoretical amount of distilled water

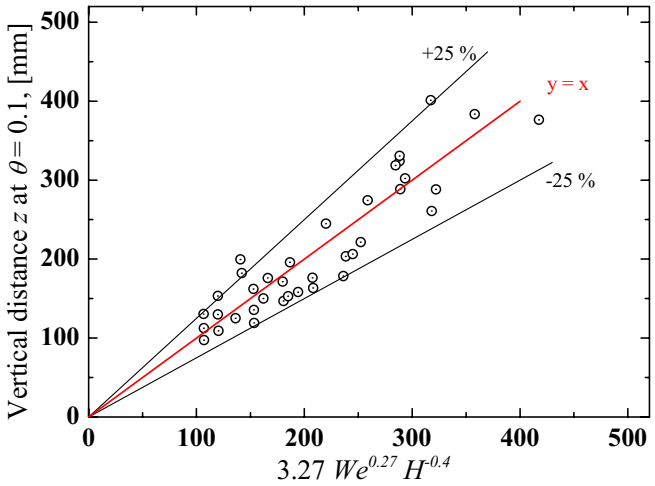

Fig. 7 Correlation of the height z, at which θ declines to the value 0.1 (At this level, evaporation is assumed to be complete)

E. Correlation of Evaporation Completion Height

Estimation of the height z at which θ declines to the value of 0.1 aims to provide the designers with the nominal height of required for the design of evaporation chamber; however, the design height should be taken above the nominal height by a suitable factor of safety. Attempts were carried out to relate the height z at which θ declines to the value 0.1 with the dimensionless numbers *We*, defined in (4) and *H* defined in (3). Equation (6) is an empirical arrangement of these dimensionless numbers to predict the height at which θ declines to the value 0.1. Fig. 7 shows that data lies within 25% of uncertainty.

$$z_{(\theta=0.1)} = 3.27\, We^{0.27}\ H^{-0.4} \tag{6}$$

VI. Investigation on Enhancement of Evaporation

Evaporation from superheated water jet happens naturally when the surrounded pressure is suddenly reduce to a value less than its saturation pressure, the previously discussed results have shown that evaporation process happens rapidly and the water attained the equilibrium conditions within several hundreds of millimeters which correspond to fraction of second after entering the depressurized area, the question which rises here is, "*Can evaporation rate be hastened somehow?*" to investigate and give an answer on the posed question, a steel mesh was installed in the way of water flow; mesh was expected to enhance the evaporation process in two aspects; dispersing the coherent water bundle near the outflow bore "*potential core zone*" and scattering the water drops into smaller spray to extend the evaporation interfacial area, through this part of study, discussion will be made on a series of results collected by experiments using meshes of different opening size and installed at three different locations with respect to nozzle exit.

A. Mesh installed just at the nozzle exit

Two stainless steel meshes of 2.5 mm and 5.0 mm square openings size were individually experimented, mesh was fixed just on the nozzle exit "*zero level*" and placed between two

Fig. 8 Top and side view of nozzle with mesh installed

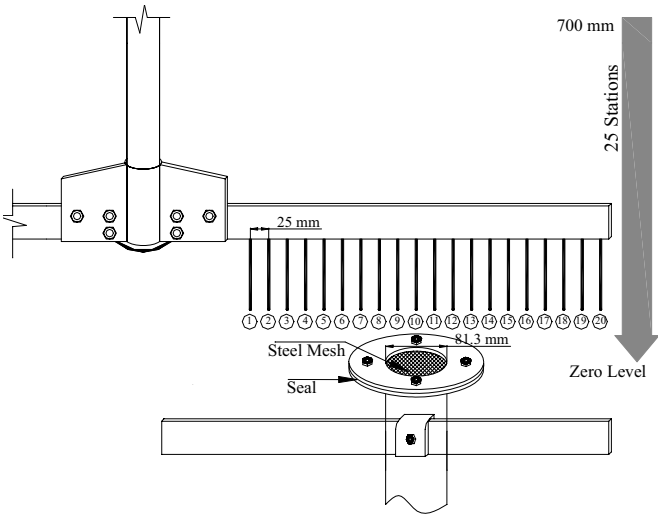

Fig. 9 Schematic diagram of nozzle with mesh installed on the exit

ring gaskets of same pipe's internal diameter to prevent leakage and both mesh and gaskets were pressed between two stainless steel hollow disks with the lower disk welded to the nozzle and the upper one attached by bolts. Photo of nozzle with mesh installed at the exit is shown in Fig 8. Fig. 9 shows schematic diagram of nozzle and the twenty platinum resistance thermometers (PRTs) fixed at intervals of 25 mm. mesh effect will be discussed through the comparison between the results of temperature profile at the centerline of the jet when mesh is installed and the corresponding profiles obtained at the same conditions when mesh is not installed, the term "*reference*" will be used to refer to the case when mesh is not installed.

Pressure reading is not available at position just below the mesh but, the nearest pressure gauge was installed in the water conveying pipe about 9.2 meter far from the nozzle exit; the pressure drop due to the mesh is assumed to be the difference between pressure readings at experiments when mesh is installed and those obtained from the *reference* experiments. This assumption is justified that the summation of head losses in the conveying pipe remains constant at same conditions unless mesh was used. From fig. 10, the pressure drop related to the mesh can be found from the difference between the curves correspond to each mesh and the reference curve where no mesh was used, as shown in this figure, pressure drop due to mesh use is negligible at low flow velocity while it

increases exponentially with velocity increase; however, the consequent pressure drop is so far independent of mesh size.

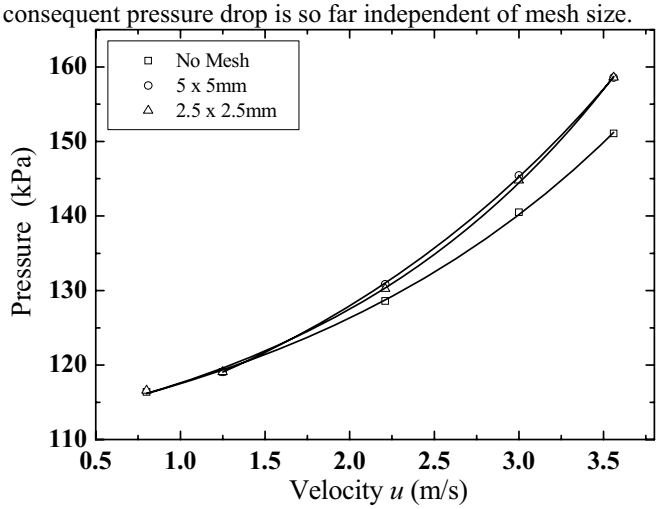

Fig. 10 Pressure drop caused by meshes placed just at the nozzle exit

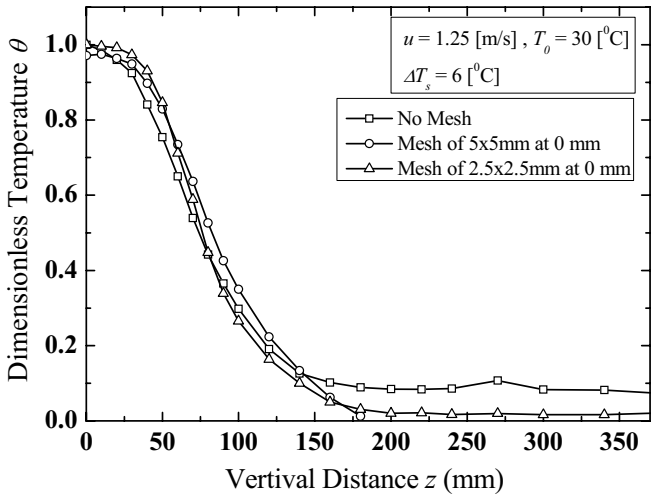

Fig.11 Influence of mesh just at the nozzle exit

Although the potential core zone near the nozzle exit is very short as in Fig.11 but the mesh results in increase the length of this zone at low velocities, this behavior is associated to the increase of effective flow velocity due to the reduction of net area of the nozzle by the mesh wires. Nevertheless, initial value of θ is larger when mesh is used and this also can be explained as a result of pressure increase in the nozzle below the mesh and delaying the achievement of superheat condition. However, reduction of the net area of the nozzle by the wires of the mesh results in increase of initial velocity just above the mesh level and subsequently the total height attained by the jet resulting in lower values of θ at the end of this zone.

B. Mesh Installed at Further Downstream Distances

To avoid the resulting pressure drop associated with mesh when it is placed just at the nozzle exit, mesh-2 was investigated at two locations of 15 and 90 mm above the nozzle exit; the schematic diagram shown in fig. 12 explains the method of placing and adjusting mesh level. As the jet diffuses in a conical shape a circular piece of mesh-2 of diameter much larger than nozzle diameter was used to ensure

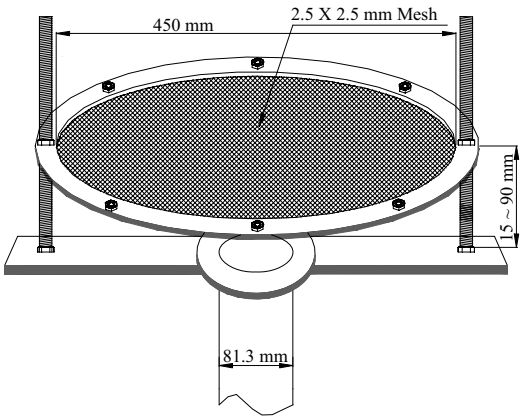

Fig. 12 schematic diagram of mesh placed above the nozzle exit

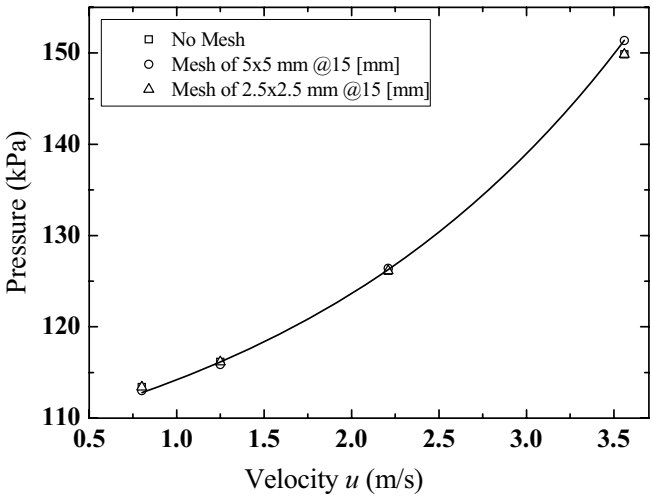

Fig. 13 Pressure drop caused by mesh located above the nozzle exit

that all water from the jet passes through the mesh.

No pressure drop was caused by mesh when it is installed at a distance as short as 15 millimeters from the nozzle exit, fig. 13 shows the pressure readings at the same point explained in fig.10, the pressure readings are so far even at high velocity.

C. Comparison between Mesh Effects at Different Locations

Figs. 14 through 17 show the temperature profiles at the centerline of the jet when mesh is installed at various locations relative to nozzle exit, in addition to the reference profile where no mesh was installed. Flow velocity still the most effective factor that governs the mesh influence; however, at velocity of 0.8 m/s, evaporation is so far unaffected by mesh at any of the three investigated locations while the influence of mesh at slightly higher velocity, 1.25 m/s is limited to the final value of liquid temperature where it declines to the lowest when mesh is installed just at the nozzle exit compared to other mesh locations as shown in fig. 15. Mesh shows considerable advantages with increase of flow velocity; as the liquid column appears near the nozzle exit is relatively long

when mesh is not used especially at higher velocities, install of mesh at few millimeters above the nozzle exit reduces the length of this coherent liquid column, this effect is associated mainly to two reasons, first is the increase of turbulence at mesh surface and the associated mixing effect and surface renewal while the second reason is the reduction of the jet inertia and momentum change due to shear forces at the mesh body along with the diffusion of water at mesh surface,

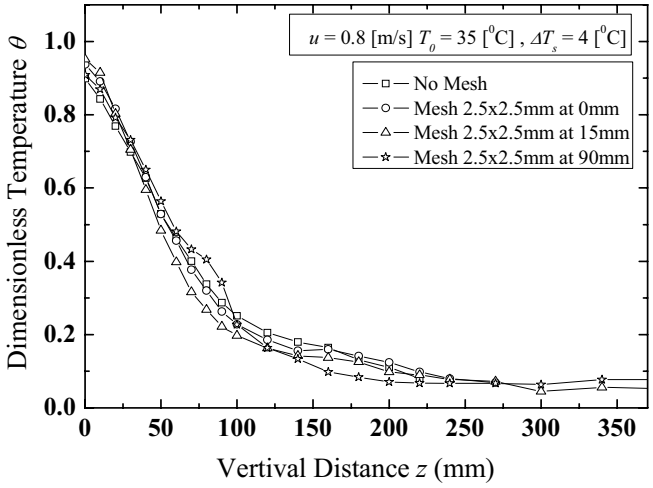

Fig. 14 Influence of mesh at various locations, u = 0.8 *m/s*

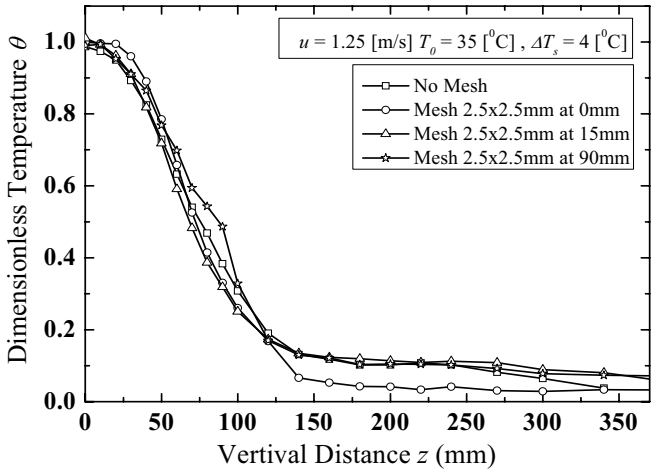

Fig. 15 Influence of mesh at various locations, u = 1.25 *m/s*

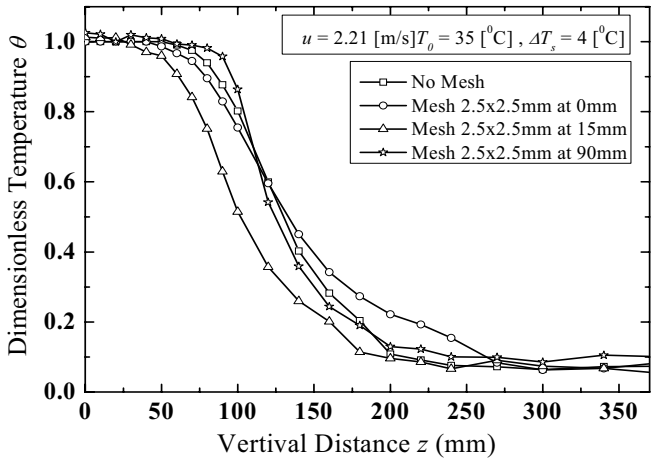

resulting in attaining lower values of θ at any vertical distance; this effect is clear in the temperature profiles when mesh is installed 15 mm above nozzle exit as shown in figs. 16 and 17 for velocities of 2.21 and 3.56 m/s, respectively.

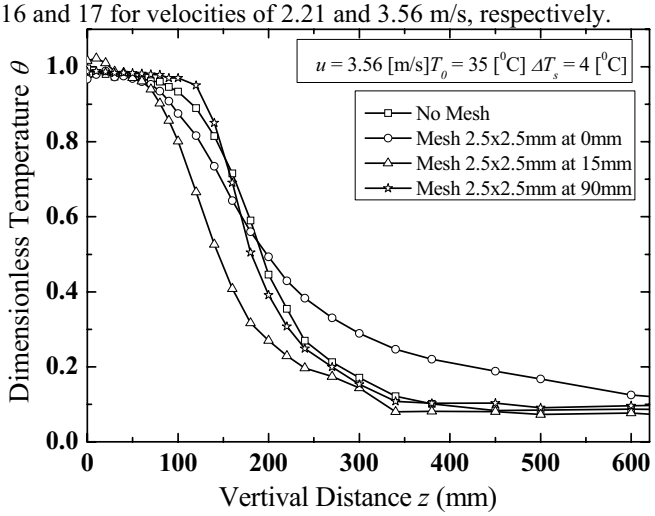

Fig. 17 Influence of mesh at various locations, u = 3.56 *m/s*

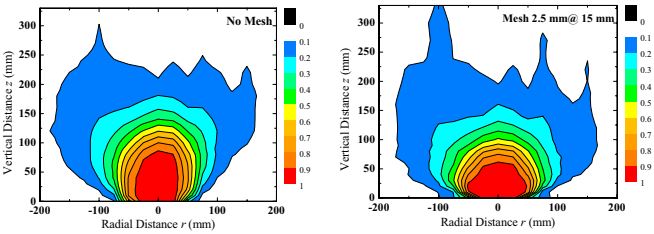

Fig. 18 Isothermal diagram show influence of mesh, u = 2.21 *m/s*.

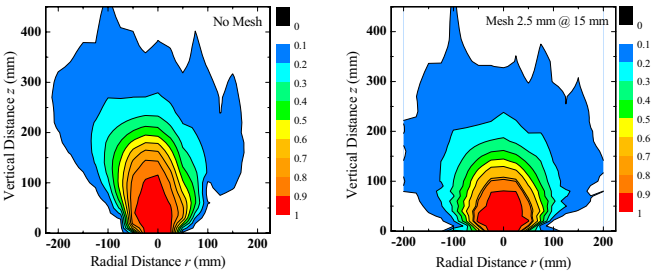

Fig. 19 Isothermal diagram show influence of mesh, u = 3.56 *m/s*.

The isothermal diagrams drown in figs. 18 and 19 show the temperature distribution at the area of influence surrounding the nozzle exit; these graphs show the influence of smaller mesh of 2.5mm square openings when it is placed 15mm above the nozzle exit at the highest two investigated flow velocities. Through these figures, it can be seen that the length of the coherent liquid column near the nozzle exit becomes shorter. The height 15mm does not mean an optimum location for mesh to be installed at, but the best of the three investigated locations; however, the optimum location of the mesh to be installed at is thought to be as close as possible to nozzle exit provided that, no pressure drop is caused.

VII. Conclusion

Experimental study on desalination by flash vaporization from superheated water jet was conducted and the following results were deduced:

Increase of flow velocity tends to maintain the jet un-shattered and cause increase of the potential core length and subsequently delay evaporation.

Within the investigated range, increase of initial water temperature was found to enhance evaporation linearly and the evaporation completion height is a function of both thermal and dynamic properties of the flow.

Mesh influences evaporation rate non-uniformly when placed at nozzle exit, while it hasten evaporation when placed slightly above the exit with no resulting pressure drop.

References

[1] O. Miyatake, T. Tomimura, Y. Ide and T. Fujii, "An Experimental Study of Spray Flash Evaporation" *Desalination*, 1981. 36(2), pp. 113-128.

[2] O. Miyatake, T. Tomimura, Y. Ide, M. Yuda and T. Fujii, "Effect of Liquid Temperature on Spray Flash Evaporation" *Desalination*, 1981. 37(3), pp. 351-366.

[3] H. Uehara, Y. Ikegami and N. Hirota, "Experimental study of spray flashes evaporation for desalination and otec" *Solar Engineering*, pp. 197-201.

[4] Y. Ikegami, H. Sasaki, T. Gouda, H. Uehara, "Experimental study on a spray flash desalination (influence of the direction of injection)" *Desalination* 194(1-3), pp. 81-98.

[5] A.E. Muthunayagan, K. Ramamurthi, J.R. Paden, "Modeling and experiments on vaporization of saline water at low temperature and reduced pressure" *Applied Thermal Engineering*, 25 (5-6), pp. 941-952.

[6] E. Mhina Peter, T. Akira and H. Yujiro, "Flashing and shattering phenomena of superheated liquid jets" *JSME Int. J*., 1994. 37(2), pp. 313–321.

[7] R. Brown, J.L. York, "Sprays formed by flashing liquid jet" *AIChE* 1962, J.8, pp. 149–153.